Fuel 88 (2009) 806–816

Contents lists available at ScienceDirect

Fuel

journal homepage: www.elsevier.com/locate/fuel

Optimization of coal-fired boiler SCRs based on modified support vector machine models and genetic algorithms

Fengqi Si [a], Carlos E. Romero [b,*], Zheng Yao [b], Eugenio Schuster [b], Zhigao Xu [a], Robert L. Morey [c], Barry N. Liebowitz [d]

[a] School of Energy and Environment, Southeast University, Si Pai Lou No. 2, Nanjing 210096, PR China
[b] Energy Research Center, Lehigh University, 117 ATLSS Drive, Bethlehem, PA 18015, USA
[c] AES Cayuga, LLC, 228 Cayuga Drive, Lansing, NY 14882, USA
[d] New York State Energy Research and Development Authority, 17 Columbia Circle, Albany, NY 12203, USA

ARTICLE INFO

Article history:
Received 25 June 2008
Received in revised form 3 October 2008
Accepted 18 October 2008
Available online 21 November 2008

Keywords:
Coal-fired boiler
Multi-objective combustion optimization
Adaptive learning
Genetic algorithms

ABSTRACT

An integrated combustion optimization approach is presented for the combined considering the trade offs in optimization of coal-fired boiler and selective catalyst reaction (SCR) system, to balance the unit thermal efficiency, SCR reagent consumption and NO_x emissions. Field tests were performed at a 160 MW coal-fired unit to investigate the relationships between process controllable variables, and optimization targets and constraints. Based on the test data, a modified on-line support vector regression model was proposed for characteristic function approximation, in which the model parameters can be continuously adapted for changes in coal quality and other conditions of plant equipment. The optimization scheme was implemented by a genetic algorithm in two stages. Firstly, the multi-objective combustion optimization problem was solved to achieve an optimal Pareto front, which contains optimal solutions for lowest unit heat rate and lowest NO_x emissions. Secondly, best operating settings for the boiler, and SCR system and air preheater were obtained for lowest operating cost under the constraints of NO_x emissions limit and air preheater ammonium bisulfate deposition depth.

1. Introduction

Utilities have a variety of methods for reducing nitrogen oxide (NO_x) emissions from existing boilers, and achieving compliance with strict federal and state regulations in the US for NO_x. These methods range from low-NO_x burner retrofitting to using post-combustion controls, such as selective catalytic reduction (SCR) systems. SCR is generally the most expensive method for NO_x emissions control, but is also the most effective. However, stringent state implementation plan (SIP) Call NO_x mandates, have motivated widespread planning for retrofitting approximately 100 GW of coal-fired capacity in the US [1]. NO_x SIP Call requirements provide incentive for designing and operating SCR process equipment to consistently achieving 90% NO_x removal, in most of the cases, year-round. Achieving high levels of SCR NO_x removal performance over a long-term period is challenging. Several investigators have shown how key SCR process variables, such as flue gas temperature and the level of reagent conditioning affect SCR performance. SCR systems are commonly designed to work with liquid anhydrous ammonia (NH_3) and aqueous NH_3, where the NH_3 reacts with the NO_x in the flue gas, reducing the oxides to molecular nitrogen and water. Although, the SCR catalyzed chemical reactions are very efficient, a small portion of the reagent does not react and leaves the reactor as "NH_3 slip." Slippage problems increase as the SCR catalyst ages and the catalyst surface become masked or plugged with fly ash. When this happens, the required NH_3 slip increases, resulting in boiler air preheater (APH) fouling by ammonium/sulfur salts. Controlling and mitigating APH fouling is imperative in coal-fired boilers, since that air handling limitations and corrosion preclude continued operation of the unit, requiring unit shutdown for APH cleaning, with the associated lost in unit availability and financial losses.

During the last few years, the ever-increasing demand for cost-efficient power generation and stringer environmental regulation has motivated implementation of process optimization strategies in coal-fired power generations. Given that coal is an important element in the energy source portfolio in the US, process optimization for stack emissions reductions and efficiency improvements in coal-fired boilers plays an important role in minimizing operational & maintenance (O&M) costs, and maximizing performance and unit availability. One area that has received significant attention is tuning and optimization of the combustion process for NO_x emissions and unit thermal performance improvement. There is a large list of reported experiences where combustion optimization has

* Corresponding author. Tel.: +1 610 758 4092; fax: +1 610 758 5959.
E-mail address: cerj@lehigh.edu (C.E. Romero).

0016-2361/$ - see front matter © 2008 Elsevier Ltd. All rights reserved.
doi:10.1016/j.fuel.2008.10.038

proved to be an effective method to reduce NO_x emissions, while mitigating its impact on the net unit heat rate [2]. With the growing population of SCR systems already retrofitted and projected to be retrofitted in the US, an expansion of combustion optimization techniques to include the combined boiler combustion/SCR system/APH is worth exploring.

An integrated optimization scheme is proposed for optimal operation of a coal-fired boiler equipped with a SCR system and rotating APHs. The optimization approach is based on having available monitoring tools for measurements of combustion-related parameters such as excess O_2 at the boiler outlet, coal flow rates overfire (OFA) register positions, etc., as well as SCR performance efficiency and APH formation of ammonium bisulfate salts (ABS). The approach is based on modified AOSVR for adaptive learning, and a GA based on non-dominated sorting GA II (NSGA-II) for implementation of the multi-objective optimization. A description of SVMs and the proposed modified AOSVR algorithm is provided, as well as of the proposed GA algorithm. The approach is built based on a case study performed at a 160 MW coal-fired boiler, firing Eastern US bituminous coal and equipped with a two layers SCR catalyst reactor. Parametric testing was performed at this unit to develop a representative database that characterize the response of NO_x emissions, NH_3 required conditioning, SCR efficiency, ABS deposition and unit heat rate penalty to changes in boiler, SCR and APH control settings.

2. Modified AOSVR and genetic algorithms

2.1. Modified AOSVR

Process modeling for boiler optimization is a key component in an optimization scheme. Modeling methods mainly fall into three categories: theoretical, data-driven and hybrid. On the basis of first-principles, combined computational fluid dynamics (CFD)/chemical kinetics models are useful for simulation and theoretical analysis [3–5]. Because historical data are available, data-driven models have become very popular, including classical statistics methods, such as principle component analysis (PCA), independent component analysis (ICA) and partial least square (PLS) [6,7], and modern artificial intelligent (AI) techniques, such as neural network (NN) and fuzzy logic [8–10]. Hybrid methods that involve first-principles and data-driven techniques have also been reported [11,12].

It is challenging to model the emissions formation process, due to its nonlinear and time-varying characteristics. A detailed approach involving first principles is computationally prohibited. AI techniques often suffer from slow training, local minima and poor interpretability. Moreover, process relationships for boilers can change with parameters, such as coal quality, slagging/fouling deposits and the conditions of the plant firing system, which can not be directly included in functional relationships due to the absence of on-line monitoring techniques. This implies that model accuracy and adaptivity are critical issues to be addressed. A modification of accurate on-line support vector regression (AOSVR) provides an avenue adaptive learning for the relationships between targets and operational variables. AOSVR is a variant of support vector machines, a supervised learning method universally used to approximate a multivariate function to any desired degree of accuracy [13–15].

2.1.1. SVR

SVR transfers an input space to a high dimension feature space in which an original nonlinear relationship can be approximated by a linear function f:

$$f(\mathbf{w},\mathbf{x}) = \langle \mathbf{w}, \Phi(\mathbf{x}) \rangle + b \tag{1}$$

where $\langle ..,. \rangle$ is an inner product, b is a threshold, $\mathbf{w} \in R^m$ is a weight vector, and Φ is a nonlinear map. Given a set of training samples $\{(\mathbf{x}_i, y_i)\}_{i=1}^{l}$, under the ε-insensitive loss [13], SVR solves:

$$\min_{\mathbf{w},b,\xi,\xi^*} \left\{ \frac{1}{2}||\mathbf{w}||^2 + C\sum_{i=1}^{l}(\xi_i + \xi_i^*) \right\}$$
$$\text{s.t.} \begin{cases} y_i - \langle \mathbf{w}, \Phi(\mathbf{x}_i) \rangle - b \leqslant \varepsilon + \xi_i \\ \langle \mathbf{w}, \Phi(\mathbf{x}_i) \rangle + b - y_i \leqslant \varepsilon + \xi_i^* \\ \xi_i, \xi_i^* \geqslant 0 \end{cases} \tag{2}$$

where C is a regularization constant, and ξ_i and ξ_i^* are slack variables [14]. The dual set of (2) is

$$\max_{\alpha,\alpha^*} \left\{ -\frac{1}{2}\sum_{i,j=1}^{l}(\alpha_i - \alpha_i^*)(\alpha_j - \alpha_j^*)K(\mathbf{x}_i, \mathbf{x}_j) - \varepsilon\sum_{i=1}^{l}(\alpha_i + \alpha_i^*) + \sum_{i=1}^{l} y_i(\alpha_i + \alpha_i^*) \right\}$$
$$\text{s.t.} \quad \sum_{i=1}^{l}(\alpha_i - \alpha_i^*) = 0, \alpha_i, \alpha_i^* \in [0, C] \tag{3}$$

where K is a kernel function determined by Φ, and α_i and α_i^* are the Lagrange multipliers. The function in (1) becomes

$$f(\mathbf{x}) = \sum_{i=1}^{l} \theta_i K(\mathbf{x}, \mathbf{x}_i) + b, \theta_i = \alpha_i - \alpha_i^* \tag{4}$$

2.1.2. AOSVR

Special optimization algorithms are necessary for SVR. Particularly, sequential minimal optimization is well suited for time-unvarying batch-wise training [16–18]. However, it is inefficient for time-varying systems, because the entire training set must be re-used while a new sample is added. An AOSVR algorithm is an alternative in which efficient updating of the support vectors is performed, whenever a new sample is added or an existing sample is removed [15]. Adding and removing the training set are conducted by Algorithm 1 (incremental) and Algorithm 2 (decremental), given that the training set is divided into three subsets E, S and R, where

$$E = \{(\mathbf{x}_i, y_i) : |\theta_i| = C\} \quad \text{(error support vectors)} \tag{5}$$
$$S = \{(\mathbf{x}_i, y_i) : 0 < |\theta_i| < C\} \quad \text{(margin support vectors)} \tag{6}$$
$$R = \{(\mathbf{x}_i, y_i) : |\theta_i| = 0\} \quad \text{(remaining samples)} \tag{7}$$

Algorithm 1. An incremental algorithm given a new sample $(\mathbf{x}_{new}, y_{new})$

1. Set $\theta_c = 0$.
2. Choose $\Delta\theta_c$ according to [15].
3. Update the θ_i of all samples and simultaneously update E, S and R.
4. If $(\mathbf{x}_{new}, y_{new}) \notin E \cup S$, then return to Step 2.

Algorithm 2. An decremental algorithm given an existing sample $(\mathbf{x}_{old}, y_{old})$

1. If $(\mathbf{x}_{old}, y_{old}) \in R$, then remove it and stop.
2. If $(\mathbf{x}_{old}, y_{old}) \notin R$, then remove it and start a circle in a reverse direction of Algorithm 1 that ends until its coefficient reduces to zero and the Karush–Kuhn–Tucher conditions [14] are still satisfied in the remaining samples.

2.1.3. Modified AOSVR

An original AOSVR model is adaptively updated by continuously adding a new sample or removing an existing sample. The first-in-first-out (FIFO) sample updating is sufficiently enough and reasonable for time series prediction and it has performed well in many applications [15]. However, the FIFO criterion can not work well when the new sample inputs are possibly controlled in a limited range, when a system continuously runs at certain conditions.

For the purpose of improvement, consider a subset of training samples with similar inputs

$$D_1 = \{(\mathbf{x}_i, y_i) : \|\mathbf{x}_i - \mathbf{x}_{\text{new}}\| < a, i = 1, \dots N\} \tag{8}$$

where a is a threshold. Another choice is

$$D_2 = \bigcap_{j=1}^{m} \{(\mathbf{x}_i, y_i) : |x_{i,j} - x_{\text{new},j}| < a_j\} \tag{9}$$

where a_j is the threshold for component j of an input vector. Input components are differentiated in D_2, at the expense of an added computing load. The subset D_1 or D_2 rather than the entire training set will be checked to obtain the sample to be removed. Specifically, a new sub-FIFO criterion is defined as follows: If D_1/D_2 is empty, then no sample is removed and otherwise the oldest sample in D_1/D_2 is removed.

2.2. Genetic algorithms

A multi-objective optimization (MOO) problem can be formulated as:

$$\begin{aligned} &\min f(\mathbf{x}) = [f_1(\mathbf{x}), f_2(\mathbf{x}), \dots, f_k(\mathbf{x})] \\ &\text{s.t.} \quad \mathbf{g}(\mathbf{x}) \leqslant 0 \\ &\mathbf{h}(\mathbf{x}) = 0 \end{aligned} \tag{10}$$

where $\mathbf{x} = [x_1, x_2, \dots, x_n]^T$ is a vector of decision variables in the decision space $\mathbf{X}$, $f_i{:}R^n \to R$ is an objective function, $i = 1, 2, \dots, k$, and $\mathbf{g}(\cdot)$ and $\mathbf{h}(\cdot)$ are the inequality and equality constraint vectors. The MOO problem is defined to find the particular set, $\mathbf{x}^* \in \mathbf{X}$, which satisfies both constraints and yields the optimal values of all objective functions. Since there is rarely a single point that simultaneously optimizes all object functions, a Pareto optimum is defined to look for trade-offs in these objectives. In this case, $\mathbf{x}^* \in \mathbf{X}$ is Pareto optimal, given any $\mathbf{x} \in \mathbf{X}$, $f_i(\mathbf{x}^*) \leqslant f_i(\mathbf{x})$, $\forall i$, and $\exists j$ with $f_j(\mathbf{x}^*) < f_j(\mathbf{x})$, and $j \in \{1, 2, \dots, k\}$. The Pareto optimal set is $S = \{\mathbf{x} \in \mathbf{X}{:}\mathbf{x}$ is Pareto optimal$\}$ and the Pareto front is $F = \{f(\mathbf{x}){:}\mathbf{x} \in S\}$.

Boiler optimization, specifically, for combined combustion and SCR system, involves multi-objectives. To deal with this MOO problem, multiple objectives can be converted into a single composite function, by assigning weights to each objective or by keeping only one objective, while putting the remainder into the constraint set. As an alternative, a representative subset can be determined in which optimal solutions are non-dominated to each other [19].

Evolutionary algorithms (EAs) are stochastic optimization methods inspired by the theory of evolution [20,21]. The process of natural evolution is simulated in an EA. A genetic algorithm (GA) is a heuristic search that derives its behavior from the natural selection theory. GAs and EAs have shown to be powerful and effective optimization methods for many real applications [22,23]. A vector evaluated algorithm was first used to solve MOO problems by Schaffer [24], and then several GA algorithms were developed with different strategies within the algorithms, such as the fitness assignment procedure, elitism and diversity mechanism [25]. The niched Pareto genetic algorithm (NPGA) was proposed to find the Pareto optimal set [26], in which a larger number of individuals are involved in competition. The non-dominated sorting genetic algorithm (NSGA) was proposed by Srinivas et al. [27] to find multi-Pareto-optimal solutions. An improved variant, NSGA-II, was presented by Deb et al. [28] (see Algorithm 3). In NSGA-II, the fast non-dominated sorting (FNS) is used to achieve a higher efficiency. The crowded tournament selection operator is used to preserve the diversity among non-dominated solutions, which can be described as: for solutions in the same non-dominated front, the solution with larger crowding distance is the winner. This avoids tuning of some parameters, usually not an easy task due to their complex interactions. Elitism is also introduced to generate a new parent population through selecting individuals from the combined population of the current parent population and its child population.

Algorithm 3. Non-dominant sorting genetic algorithm II (NSGA-II)

1. Set $t = 0$ and start with a random initial population P_t of size N.
2. Create an offspring population Q_t of size N by crossover and mutation.
3. Combine P_t and Q_t into $R_t = P_t \cup Q_t$.
4. Apply the FNS method and identify non-domination fronts F_1, $F_2, \dots, F_k$ in R_t.
5. Assign fitness according to the crowing distance.
6. Select individuals for P_{t+1}. For $i = 1, 2, \dots, k$, run: if $|P_{t+1}| + |F_i| \leqslant N$, then $P_{t+1} = P_{t+1} \cup F_i$ and otherwise add the first $(N - P_{t+1})$ solutions of F_i to P_{t+1}.
7. Apply crossover and mutation to P_{t+1} for a new offspring Q_{t+1}.
8. Return if the stopping condition is satisfied, otherwise $t = t + 1$ and go to Step 3.

3. Unit testing

3.1. Unit description

An optimization scheme, based on AOSVR for adaptive learning and GAs for constrained optimization, was applied to field test data obtained from a 160 MW coal-fired utility boiler. Field data were acquired from a parametric test program performed at a 160 MW coal-fired boiler. The test boiler is of a tangentially fired combustion engineering (CE) design, equipped with a low-NO_x concentric firing system (LNCFS) level III. The LNCFS-III system consists of four elevations of burners arranged in corners. Fig. 1 displays a diagram of the test unit. Four pulverizers (1A1, 1B2, 1A3 and 1B4, from top to bottom) supply coal to the burner system, one mill per elevation. The windbox compartment at each corner is composed of coal air registers for tertiary air (coaxial with the burner nozzle), auxiliary air registers and concentric fire system (CFS) air registers that are used to divert combustion secondary air at an offset, with respect to the burner centerline. In addition to the mentioned secondary air ports, the LNCFS-III arrangement incorporates OFA in two sets of registers, a two-level close-couple overfire air (CCOFA) register set, and a separated OFA (SOFA) compartment above the burner zone with three-level registers. All the burner buckets and CCOFAs are connected to tilt in unison for controlling of steam temperatures. The SOFA compartments are also tiltable for combustion staging.

The test boiler is equipped with a 2-layer, anhydrous NH_3-based SCR system, with a total catalyst volume of 164 m^3 for additional NO_x control. The SCR system is equipped with NO_x analyzers at the inlet and outlet of the reactor, and an ABS monitoring sensor, manufactured by Breen Energy Inc. The Breen Energy's AbSensor – AFP is a probe that measures the conduction of electrical current across the probe's tip that results from condensed hydrated ammonium bisulfate. The instrument reports both the ABS formation and evaporation temperature via OLE for process control (OPC). The rest of the boiler back-end configuration includes two rotating APHs with air bypass dampers, an electrostatic precipitator for particulate removal, and a flue gas desulphurization unit.

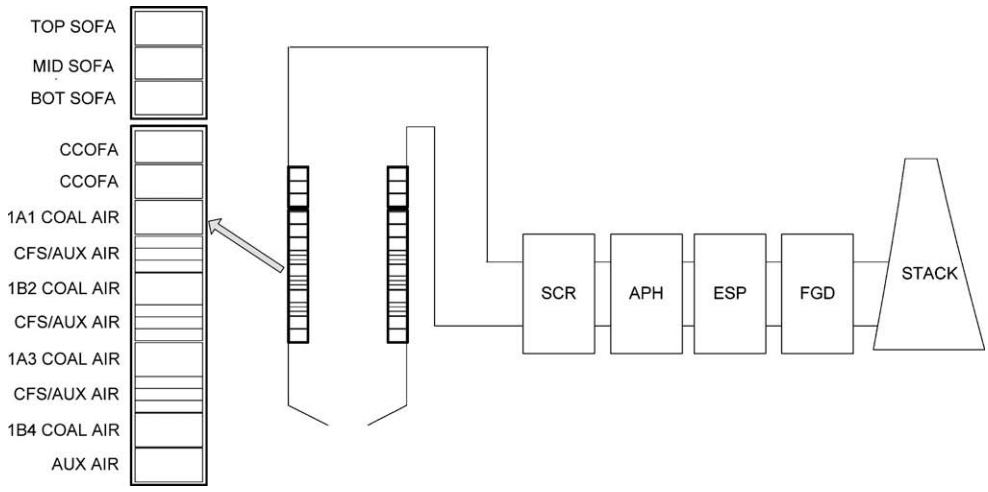

Fig. 1. Schematic of test unit.

3.2. Parametric field tests

Parametric field tests were performed at the test unit, with data collected at different combinations of boiler firing system, SCR and APH operational settings, at steady-state conditions. All tests were performed at full load, which was appropriate for this unit, since it is a base-loaded unit. The parameters used for testing and their available operating ranges are included in Table 1. Economizer excess O_2, was used as an indication of the amount of excess air fed to the boiler, the average of the top and middle SOFA register openings was used as an indication of combustion staging. Additionally, the average burner and tilt angles, and the coal flow rate to the top 1A1 mill were included in the parametric list to characterize the relationship between boiler control settings and boiler outlet or SCR inlet NO_x and unit thermal performance. Other parameters used to characterize the parametric relationships at the SCR and APH include the NH_3 flow rate and the APH bypass damper position, respectively. The parametric testing was conducted by changing individual parameters at a time, while keeping the setpoints of the other parameters constant during each test period. A total of 80 parametric tests were performed at full unit load. These tests were performed according to a design of experiment based on the number of input parameters. During testing, each parameter in Table 1 was changed within a reasonable range and a database of pertinent data was acquired from the plant PI system at a sampling rate of each minute. Fly ash was sampled for each test run and analyzed off-line for unburned carbon or loss on ignition (LOI). For some of these ash samples, ammonia in ash was also determined by analysis. Results are listed in Table 2. Data on SCR inlet and outlet, and SCR efficiency (defined as the normalized NO_x reduction across the SCR with respect to the inlet NO_x), main steam and hot reheat steam temperatures, attemperating flow rates, flue gas and air temperatures across the different equipments in the convective pass, and fly ash unburned carbon level were acquired for each test point. Indication of the net unit heat rate penalty for each test point, or combination of test parameters, with respect to design conditions, was provided by a heat and mass balance model of the unit [29].

During parametric testing, a unit outlet NO_x emissions constraints of 7 mg/MkJ was used. Additionally, another constraint was imposed at the APH that consisted of maintaining the ABS deposition location at the APH at 0.76 m from the cold-end. This location setpoint was chosen based on the known penetration distance of the APH sootblowers, which are located at the outlet of the APH. Any deposition of sticky ABS deposits on the metal surface of the APH baskets, beyond the chosen deposition setpoint, would not

Table 1
Parametric list.

No.	Symbol	Variable description	Unit	Upper limit	Lower limit
1	O_2	Excess O_2	%	4.0	2.5
2	SOFA	Average top SOFA opening	%	100	0
3	α_{ST}	SOFA tilt	Deg.	25	−15
4	α_{BT}	Burner tilt	Deg.	1	−15
5	F_{coal}	Coal flow rate of top mill	t/h	19	0
6	NH_3	Ammonia flow rate	kg/h	250	0
7	D_{APH}	APH bypass damper position	%	100	0

Table 2
Ash analysis data.

Samples	1	2	3	4	5	6	7	8	9	10	11	12	13	14
LOI (%)	2.9	3.3	2.8	2.4	2.2	2.7	3.6	2.3	4.4	3.8	2.7	2.5	3	5.2
Amonnia in ash (mg/kg)	64.7	179.0	67.7	51.0	49.6	42.7	50.3	26.0	39.1	24.8	37.9	39.6	27.0	36.8
Samples	15	16	17	18	19	20	21	22	23	24	25	26	27	28
LOI (%)	3.9	2.6	2.5	2.7	1.6	3.5	3	3.2	3.3	3.2	3.5	3.3	5.4	10.9
Amonnia in ash (mg/kg)	39.9	27.5	27.7	19.6	10.4	16.9	20.1	22.5	20.3	16.8	19.8	17.9	20.7	62.9

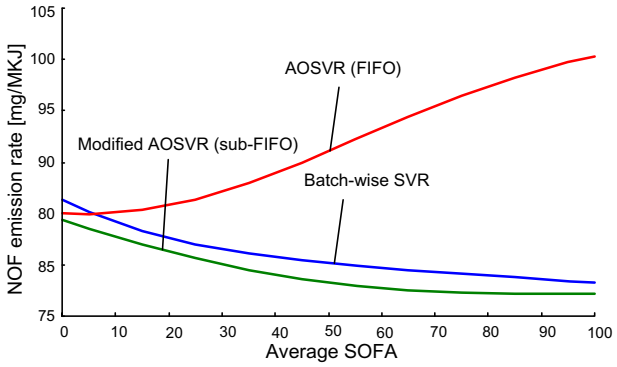

Fig. 2. Adaptive model updating results for different SVR models.

Table 3
Prediction performance of different SVR models.

	Batch-wise SVR	AOSVR(sub-FIFO)
MAE	9.92	1.65

be removed by sootblowing, increasing the risk of gradual fouling of the APH and loss of generation for APH washing [30]. The ABS deposition distance was calculated using the measured AbSensor evaporation temperature and an estimated APH metal temperature profile calculated from the code reported by Sarunac et al. [31]. The axial location of the APH metal temperature profile at which the metal temperature is equal to the ABS formation temperature establishes the ABS deposition distance from the APH cold-end. Two options are available when the ABS deposition distance is beyond the reach of the sootblowers (exceeds the 0.76 m setpoint), viz. to lower the NH_3 injection rate to the lowest conditioning permitted to achieve the required outlet NO_x level, or manipulate the APH air bypass damper to increase the metal temperatures. Opening the APH bypass damper is the least preferred option, since it results in heat rate penalties, due to the increase in the flue gas temperature exiting the boiler.

4. Results and discussion

4.1. Process models

AOSVR was used to built functional relationships between the boiler outlet or SCR inlet NO_x level and heat rate penalty (with respect to the design heat rate level), and the five boiler parameters included in Table 1 (O_2, SOFA, α_{ST}, α_{BT} and F_{coal}). To demonstrate the adaptive ability of the SVR technique, three models were studied: batch-wise SVR, conventional AOSVR based FIFO, and modified

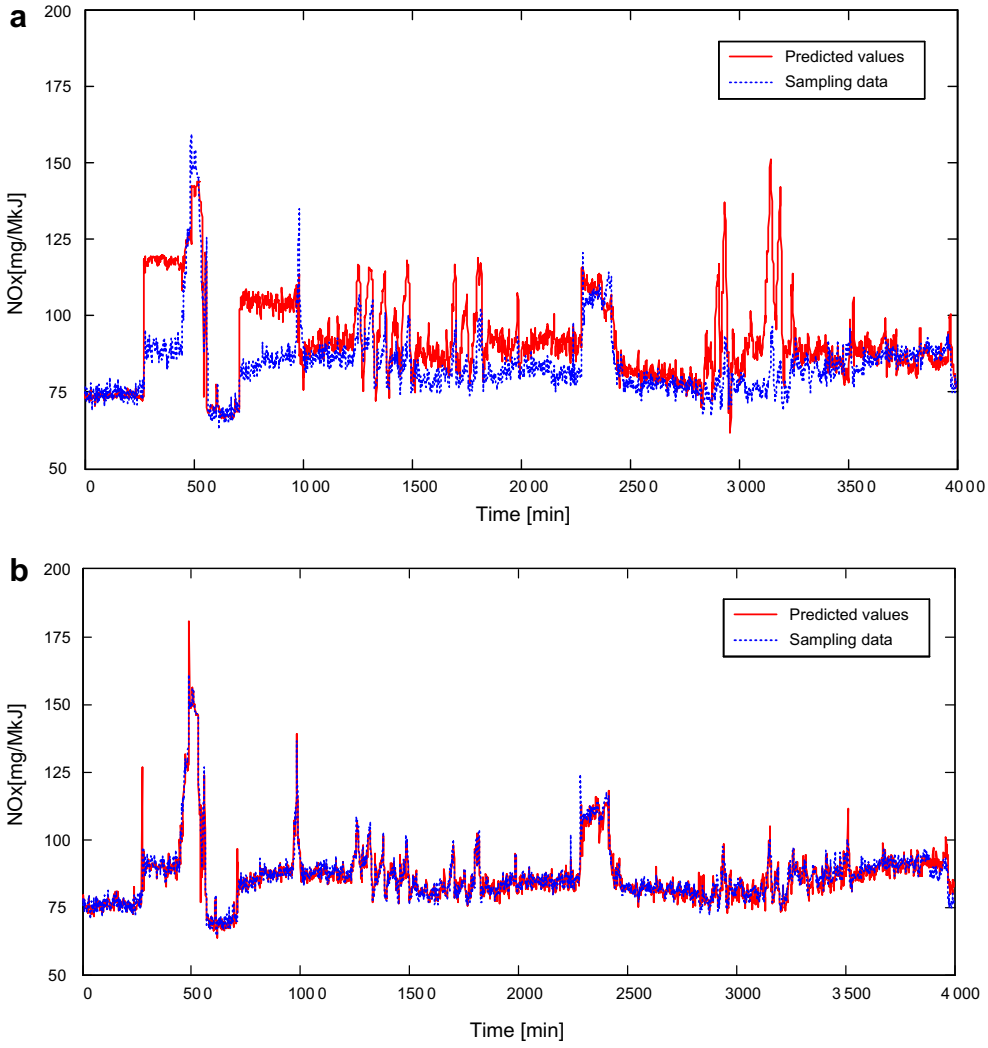

Fig. 3. Prediction of NO_x emissions: (a) batch-wise SVR and (b) modified AOSVR (sub-FIFO).

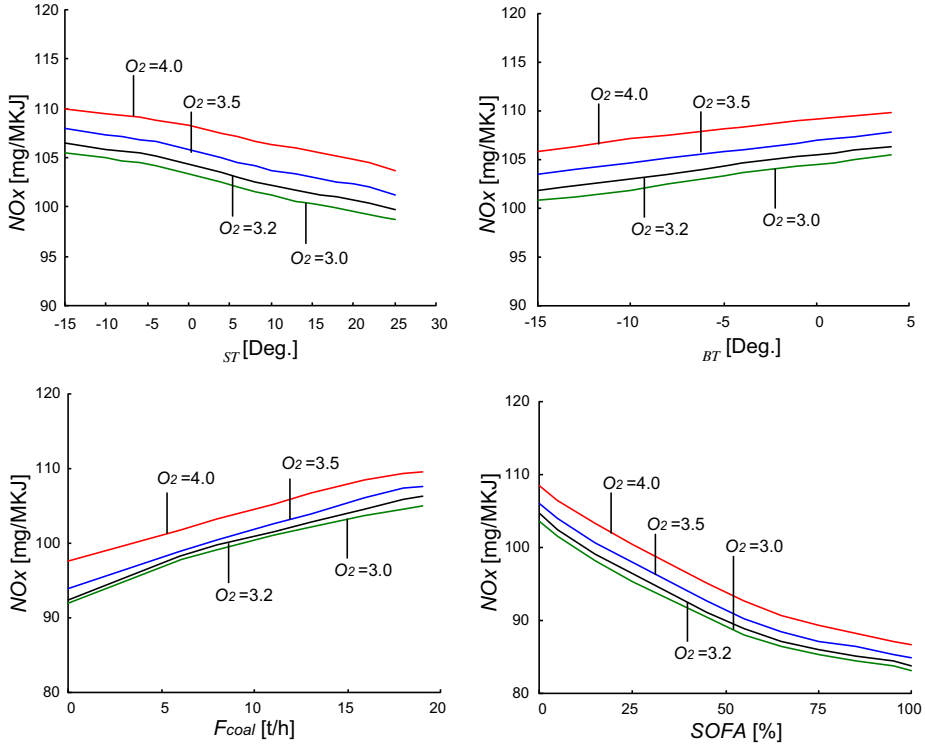

Fig. 4a. Incremental analysis results of the trained AOSVR models for SCR inlet NO_x emissions.

AOSVR based sub-FIFO. The three models were initially trained with the database obtained from the parametric tests, and then adaptively updated based on real time data sets. In this demonstration, 4000 continuous samples were acquired from the real process at a 1-min sample rate. In comparison to the batch-wise SVR, where there was no updating present, the other two models were continuously updated with every new sample. The results from the three methods for the relationship between average SOFA and SCR inlet NO_x emissions rate is shown in Fig. 2. The batch-wise SVR kept the relationship learned from the parametric tests, unchanged. Although, both AOSVR models were continuously regulated to include the new relationship existing with the new samples, the conventional AOSVR based FIFO produced a wrong trending.

The prediction performance of the batch-wise SVR and the proposed AOSVR based sub-FIFO model were further compared. Table 3 shows the predicted performance for every model, using a mean absolute percentage error (MAE) as the validation criterion, which is defined as:

$$\mathrm{MAE} = \frac{1}{n}\sum_{i=1}^{n}\frac{|y_i - \widehat{y_i}|}{y_i} \times 100\% \tag{11}$$

where n is the sample size, y_i denotes the sample data, and $\widehat{y_i}$ is the modeling output value. The batch-wise SVR exhibited the worse performance for NO_x emissions prediction, because the operational conditions were quite different than those used during the field testing. Fig. 3 shows a detailed profile of predicted values up to the 4000-min. Biases in Fig. 3a result from the difference in operating conditions and coal quality between the test conditions and those in the real process. These biases were compensated by adopting new samples to the training set in the adaptive learning mode, as shown in Fig. 3b.

The modified AOSVR based on the sub-FIFO model was chosen to develop two robust models respectively for SCR inlet NO_x and unit heat rate penalty. Both models were trained based on the field datasets. The model parameters were set as follows: the Gaussian kernel function with a width of 1.0, and the ε-insensitive loss function with $\varepsilon = 0.05$, and $C = 100$. The optimization scheme was implemented based on the trained models. Figs. 4a and 4b show trend results obtained with the trained AOSVR models for SCR inlet NO_x and heat rate penalty, respectively.

4.2. Optimization models

The constrained optimization problem for optimal operation of the combined boiler/SCR/APH was performed in two steps. In the first step, a GA was used to obtain a functional relationship between the lowest (or optimal) achievable heat rate penalty and boiler outlet or SCR inlet NO_x. This is a classic constrained multi-objective optimization problem, which was defined by

$$\begin{aligned}
&\min\ \mathrm{NO}_x = f_{\mathrm{NO}_x}(O_2, \mathrm{SOFA}, \alpha_{\mathrm{ST}}, \alpha_{\mathrm{BT}}, F_{\mathrm{coal}})\\
&\min\ q = f_q(O_2, \mathrm{SOFA}, \alpha_{\mathrm{ST}}, \alpha_{\mathrm{BT}}, F_{\mathrm{coal}})\\
&\text{s.t. } \theta = f_\theta(O_2, \mathrm{SOFA}, \alpha_{\mathrm{ST}}, \alpha_{\mathrm{BT}}, F_{\mathrm{coal}}) \leqslant \theta_{\max}\\
&O_{2,\min} \leqslant O_2 \leqslant O_{2,\max}\\
&\mathrm{SOFA}_{\min} \leqslant \mathrm{SOFA} \leqslant \mathrm{SOFA}_{\max}\\
&\alpha_{\mathrm{ST},\min} \leqslant \alpha_{\mathrm{ST}} \leqslant \alpha_{\mathrm{ST},\max}\\
&\alpha_{\mathrm{BT},\min} \leqslant \alpha_{\mathrm{BT}} \leqslant \alpha_{\mathrm{BT},\max}\\
&F_{\mathrm{coal},\min} \leqslant F_{\mathrm{coal}} \leqslant F_{\mathrm{coal},\max}
\end{aligned} \tag{12}$$

where $f_{\mathrm{NO}_x}(\cdot)$ and $f_q(\cdot)$ are the objective functions between the five boiler operating variables listed in Table 1, and boiler outlet NO_x emissions and heat rat penalty, q, respectively. $f_\theta(\cdot)$ is the function that describes the functional relationship between fly ash unburned carbon level and the boiler control settings. The optimization was constrained by fly ash unburned carbon to be below a prescribed maximum of 4%, and the operating input parameters to be between minimum and maximum levels, representing their operational upper limit and lower limit indicated in Table 1.

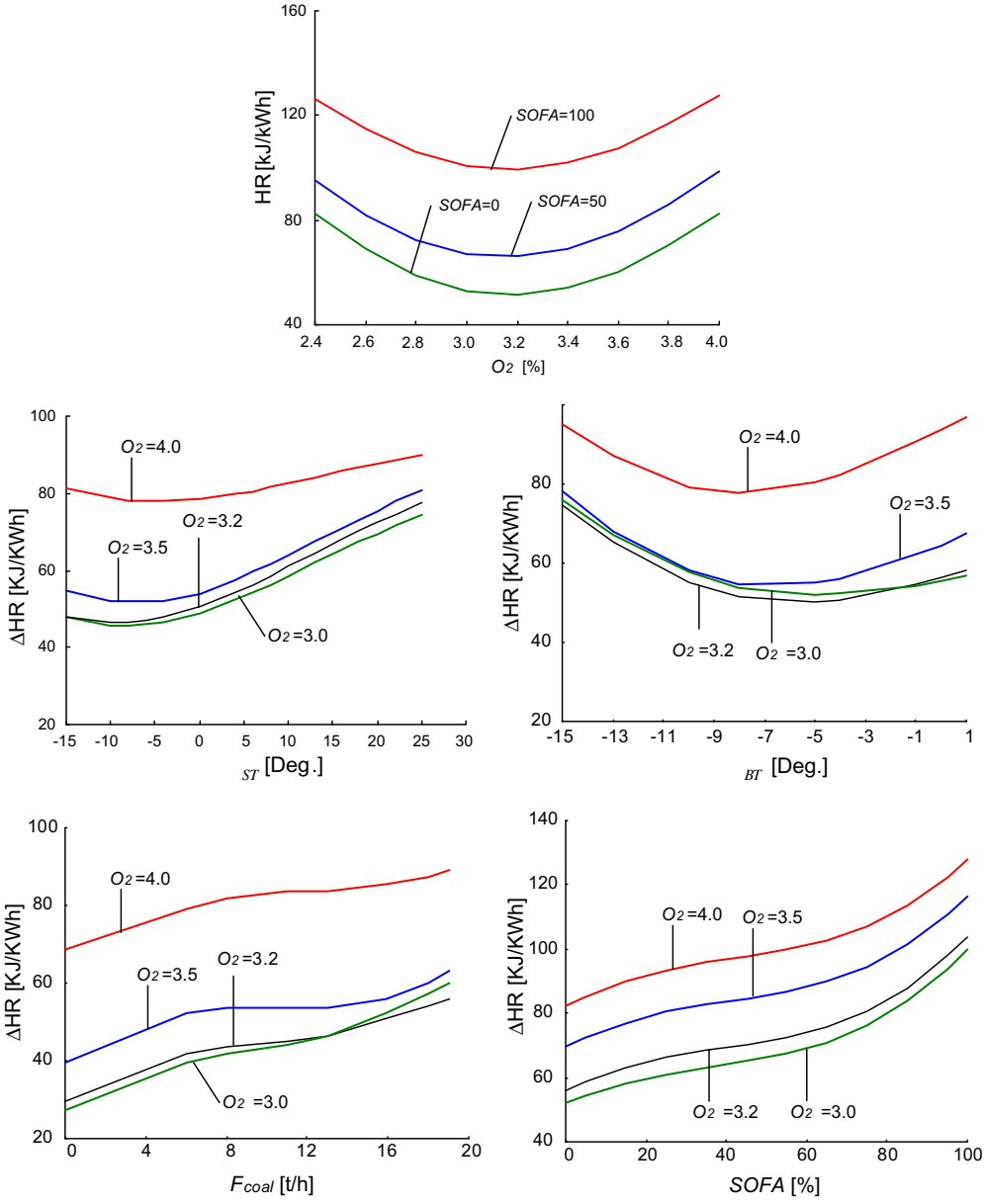

Fig. 4b. Incremental analysis results of the trained AOSVR models for heat rate penalty.

The second step of the optimization consisted of minimizing an overall cost function that combines the costs of: (1) the heat rate penalty from the boiler side, due to a combination of boiler controls settings to achieve a particular boiler outlet or SCR inlet NO_x emissions rate; (2) the cost of NH_3 to produce the maximum SCR performance to achieve a target NO_x reduction; and (3) the heat rate penalty to operate the APH within the ABS deposition constraint. Savings due to avoidance of APH washes was not included in the cost function to be optimized. The second step optimization, performed with a GA was defined by

$$\begin{aligned}
&\min\ C_{\text{total}} = k_1 C_1(\text{NO}_x) + k_2 C_2(\text{NH}_3) + k_3 C_3(D_{\text{APH}})\\
&\text{s.t. } d = g_{\text{depth}}(\text{NO}_x, \text{NH}_3, D_{\text{APH}}, SO_2, T_{\text{gas, inlet}}, T_{\text{gas, outlet}}, T_{\text{air, inlet}}, T_{\text{air, outlet}}) \leqslant a_{\text{depth}}\\
&\text{NO}_{x,\text{outlet}} \leqslant a_{\text{NO}_x,\text{limit}}\\
&\text{NO}_{x,\min} \leqslant \text{NO}_x \leqslant \text{NO}_{x,\max}\\
&\text{NH}_{3,\min} \leqslant \text{NH}_3 \leqslant \text{NH}_{3,\max}\\
&D_{\text{APH, min}} \leqslant D_{\text{APH}} \leqslant D_{\text{APH, max}}
\end{aligned} \tag{13}$$

where the total cost C_{total} is composed of the fuel cost, C_1, due to the boiler heat rate penalty contribution (obtained from the results of the optimization of Step 1) on optimum unit heat rate from Eq. (12), the ammonia injection cost, C_2, and the heat rate penalty cost, C_3, due to the manipulation of the APH bypass damper (D_{APH}). The coefficients k_i, i = 1,2,3 were set with a value of 1.0. The $g_{\text{depth}}(\cdot)$ is the constraining functional relationship between pertinent operating variables and the deposition depth, which was set $<a_{\text{depth}}$ = 0.76 m. The unit outlet NO_x emissions rate was constrained at $< a_{\text{NO}_x,\text{limit}} = 7$ mg/MkJ.

For the cost function, a functional relationship for the lowest NH_3 injection flow rate required as a function of SCR inlet NO_x was obtained from the parametric test data. Fig. 5 shows this relationship. At the lowest reagent conditioning, the highest SCR efficiency results, while maintaining the unit outlet NO_x emissions at the constrained limit. The minimal NH_3 vs. SCR inlet NH_3 curve shows a rapid increase when the SCR inlet NO_x level exceeds the 110 mg/MkJ level, which is characteristic of the catalyzed NO_x reduction process in the SRC reactor. Maintaining the NH_3 injection rate with the same slope as the one used for low NO_x levels (<110 mg/MkJ) would result in violation of the NO_x emissions

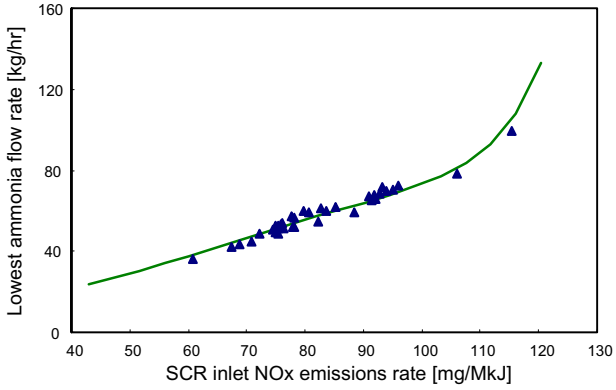

Fig. 5. Lowest ammonia flow rate vs. SCR inlet NO_x.

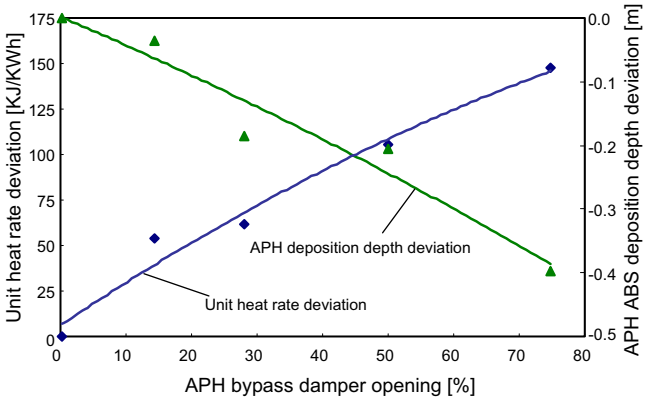

Fig. 6. ABS deposition and heat rate deviation vs. APH bypass damper opening.

constraint. Furthermore, this increase in reagent for elevated SCR inlet NO_x levels is what increases the risk of NH_3 slip and, subsequent formation of ABS in the actual SCR system.

Additionally, for the cost function, the relationship between APH air bypass damper and unit heat rate penalty was obtained from field testing at different bypass damper opening positions, resulting in different APH metal temperature profiles, and ABS deposition depths with respect to the ABS deposition location set point. Fig. 6 shows ABS depths vs. APH bypass damper position. Also included in Fig. 6 is the accompanying heat rate deviation or penalty associated with the opening of the APH bypass damper, because of the increase in APH outlet gas temperature.

Table 4
Selected solutions for the final generation.

O_2 (%)	SOFA (%)	F_{coal} (t/h)	α_{BT} (°)	α_{ST} (°)	NO_x (mg/MkJ)	ΔHR (kJ/kWh)
2.51	60	6.0	−10	24	72.3	90.3
2.61	60	6.0	−10	15	73.2	67.4
2.70	60	6.0	−10	4	75.3	48.7
2.52	60	6.0	−9	−13	77.5	37.6
2.87	60	6.0	−9	−15	79.5	32.0
2.83	49	6.0	−8	−15	81.6	31.7
2.87	35	6.0	−6	−15	85.8	30.8
2.86	21	6.0	−5	−15	90.3	30.2
2.88	10	6.0	−4	−15	94.5	29.7

4.3. Optimization results

Using the AOSVR trained models, $f_{NO_x}(\cdot), f_q(\cdot)$ and $f_\theta(\cdot)$, the optimization problem expressed by the Set (12) was solved by the NSGA-II method [28]. The model parameters were set as: population size, 240; crossover probability, 0.9; mutation probability, 0.1 and maximum generation, 30. Fig. 7a–d shows feasible solutions for the Set (12) and the set of optimal combination of boiler parameters at different levels of target SCR inlet NO_x. A sequence of Pareto front approximations can be obtained at different generations as shown in Fig. 7b–d. A converged optimal Pareto front was obtained and shown Fig. 7d, which can be taken as the best approximation of the true Pareto front of the given problem. Table 4 shows selected optimal solutions obtained at the 30th generation. These selected operating conditions and corresponding

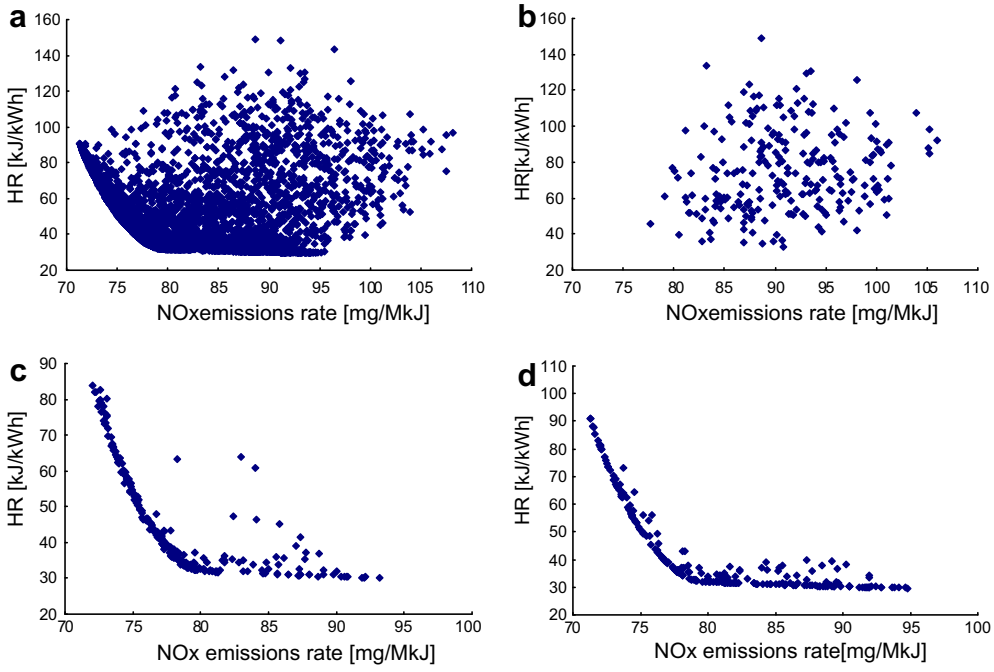

Fig. 7. Optimization results for Set (12). (a) Feasible solutions. (b) Initialization of first generation. (c) Pareto front of 15th generation. (d) Pareto front of 30th generation.

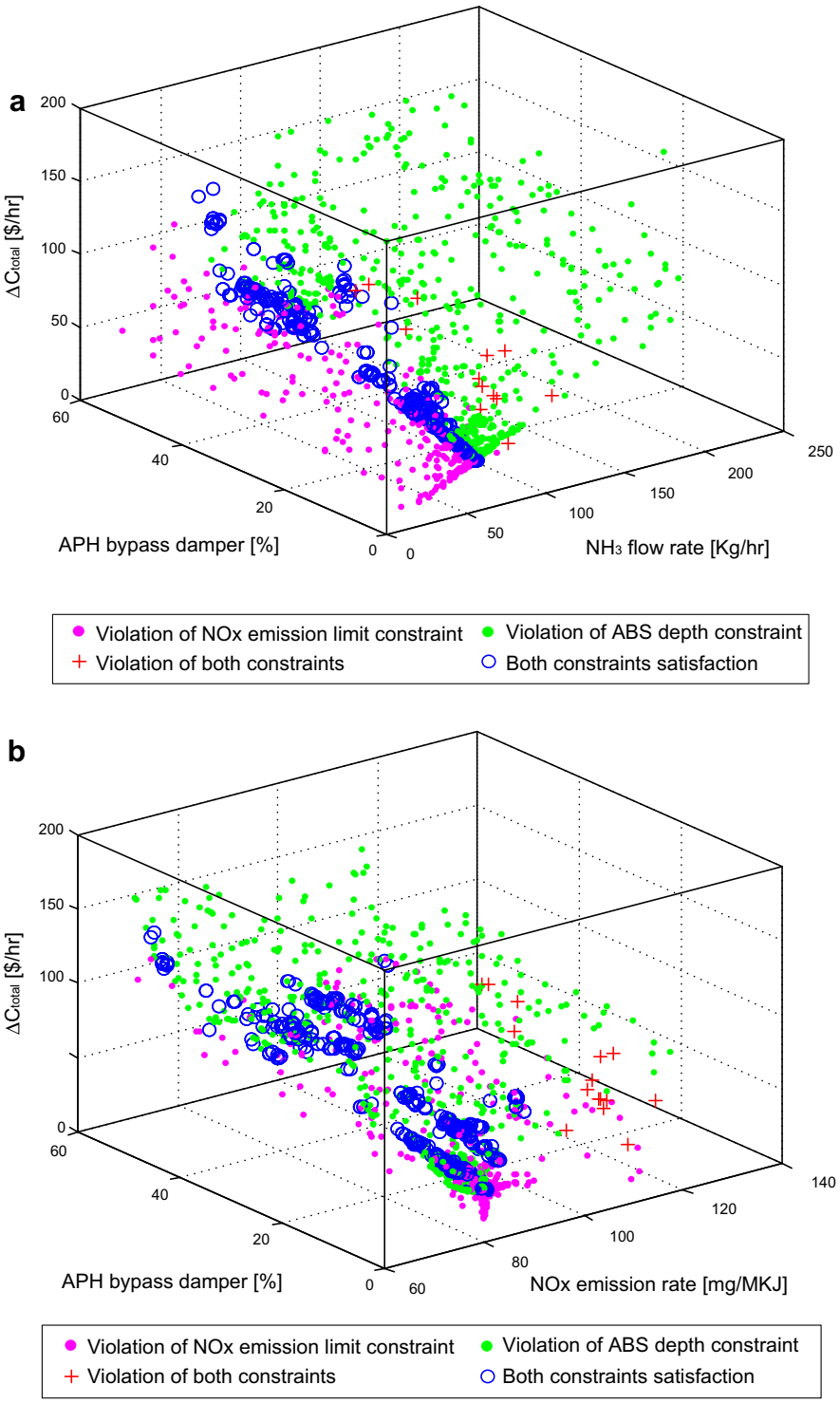

Fig. 8. GA optimization solutions for Set (13). (a) Unit operating cost vs. NH_3 and APH bypass damper. (b) Unit operating costs vs. NO_x and APH bypass damper.

NO_x emissions rate and heat rate deviations are listed in ascending order of SCR inlet NO_x.

The optimization problem expressed by the Set (13) was solved by another NSGA-II model with the following settings: population size, 180; crossover probability, 0.9; mutation probability, 0.1; and maximum generation, 22. The cost function was evaluated using the following rates: generation power cost of \$0.02/kwh and ammonia reagent cost of \$0.55/kg, to convert the objective function to units of dollars per hour. Fig. 8a and b shows a 3D map of all searched solutions by the GA. Also, included in Fig. 8a and b are the sets of SCR inlet NO_x, NH_3 injection rate and APH bypass damper positions that violate the ABS deposition distance constraint and the NO_x emissions rate limit. The set of feasible solutions, which satisfy both constraints in Set (13) are also shown in Fig. 8a and b. These solutions correspond to the optimal GA Pareto, 22th generation, which was implemented for the lowest operation cost. Fig. 8a clearly shows on the *z*-axis that a low NH_3 injection rates the outlet NO_x emissions limit constraint is violated, while at high NH_3 injection rates the ABS deposition constraint is violated. Optimal solutions that

Table 5
Optimal solutions as a function of APH ABS deposition depth.

No.	a_{depth} (m)	O_2 (%)	SOFA (%)	F_{coal} (t/h)	α_{BT} (°)	α_{ST} (°)	NO_x (mg/MkJ)	NH_3 (kg/h)	D_{APH} (%)	η_{SCR} (%)	ΔC_{total} ($/h)	C_1 ($/h)	C_2 ($/h)	C_3 ($/h)
1	0.76	2.82	52.0	6.0	−8.4	−13.7	80.6	56.7	0.0	91.3	41.2	10.1	31.2	0.0
2	0.73	2.90	50.7	6.0	−7.7	−14.9	81.7	57.5	6.0	91.4	48.9	9.9	31.6	7.5
3	0.70	2.84	50.4	6.0	−8.0	−13.4	81.1	57.0	12.6	91.4	55.2	9.9	31.4	13.9
4	0.67	2.85	42.8	6.0	−6.7	−15.0	83.5	58.7	18.9	91.6	60.5	9.4	32.3	18.8
5	0.64	2.85	42.9	6.0	−6.7	−15.0	83.4	58.6	25.2	91.6	64.3	9.5	32.2	22.6
6	0.61	2.97	40.1	6.0	−6.1	−15.0	85.1	59.7	31.1	91.8	67.4	9.1	32.9	25.5
7	0.58	2.85	50.5	6.0	−8.2	−15.0	81.3	57.2	37.4	91.4	69.5	9.9	31.5	28.1
8	0.55	2.52	60.0	6.0	−9.0	−13.0	77.4	54.3	42.7	91.0	72.2	12.2	29.9	30.2
9	0.52	2.92	41.2	6.0	−7.3	−15.0	84.1	59.1	48.7	91.7	74.2	9.3	32.5	32.4
10	0.49	2.87	60.0	6.0	−9.5	−14.7	79.3	55.7	54.3	91.2	76.0	10.6	30.7	34.8
11	0.46	2.94	34.3	6.0	−5.3	−15.0	86.6	60.8	59.5	91.9	79.3	8.7	33.4	37.2

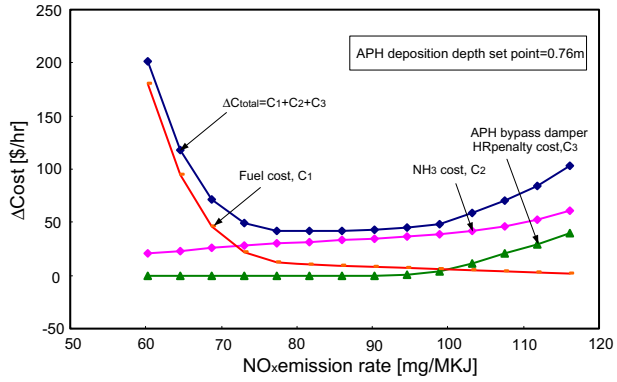

Fig. 9. Resulting costs vs. boiler outlet NO_x emissions levels.

satisfy both constraints are obtained in the NH_3 flow rate range between 55 and 90 kg/h.

The optimal solution for to the lowest cost of compliance corresponds to the following control setting: O_2 = 2.82%, average SOFA register opening = 52.0%, NH_3 injection rate = 56.7 kg/h, average burner tilt angle = −8.4°, average SOFA tilt angle = −13.7°. This combination of settings will result in NO_x emissions at the boiler outlet of 80.6 mg/MkJ, while complying with the unit outlet NO_x limit, ABS deposition of less than 0.76 m and fly ash unburned carbon below 4%, at a differential cost of $41.2/h. Table 5 shows different optimal solutions corresponding to different APH ABS deposition depths. The total cost of compliance increases as the ABS deposition distance is tightly set closer to the APH cold-end. A reduction in the ABS deposition depth setpoint below 0.76 m would require opening of the APH bypass damper, with associated heat rate penalty from this component of the cost function. Fig. 9 shows the resulting costs associated with operation a optimal combinations of boiler control settings that result in a range of boiler outlet NO_x emissions levels. It is clearly seen in Fig. 9 that the control of ammonia flow rate should be the first approach to limit the cost function to the point where the boiler heat rate penalty increases. Allowing the boiler outlet or SCR inlet NO_x to increase without control would result in additional NH_3 consumption and the need to open the APH bypass damper for ABS deposition control, with its associated cost increase due to the APH heat rate penalty.

5. Conclusions

Process optimization is a cost-effective approach to maximize profits in fossil-fired boiler, while meeting environmental limits. In coal-fired boilers equipped with SCRs, this is a classic multi-objective optimization problem to balance efficiency, NO_x emissions and maintenance. The models of real processes are the important basis for optimization schemes which are often influenced by complicated mechanisms, nonlinear time-varying characteristics, variable coal quality and cleanness of boiler heat transfer surfaces.

In this paper, a modified AOSVR model is proposed with a modified removing criterion, to decide the right samples before including them in the training. A field case study revealed the validity of this approach and its performance in both the prediction and function approximation by adaptive learning for adaptation to operating conditions variation.

An optimization model, based on the NSGA-II algorithm is used to solve the constraint optimization problem, which was implemented in two stages. In the first stage, feasible optimal solutions were obtained from a Pareto front, including the given optimal targets and the corresponding settings of control parameters. Lowest operation cost was achieved by the second stage optimization, which considers the unit heat rate penalty, as well as the cost of ammonia reagent.

Acknowledgement

Funding for this project was provided by the New York State Energy Research and Development Authority, under Contract No. 10083, and by AES Cayuga, LLC.

References

[1] Cichanowicz E, Smith L. SCR performance analysis hints at difficulty in achieving high NO_x removal targets. Power Eng 2002;106:82–90.
[2] Romero C, Sarunac N. Field results from application of Boiler OP to utility boilers. In: 43rd annual ISA POWID controls and instrumentation conference, San Antonio, TX, June 4–9; 2000.
[3] Dong W. Design of advanced industrial furnaces using numerical modeling method. Ph.D. Thesis, Department of Materials Science and Engineering, Stockholm, Sweden; 2000.
[4] Habib MA, Ben-Mansour R, Antar MA. Flow field and thermal characteristics in a model of a tangentially fired furnace under different conditions of burner tripping. Heat Mass Transfer 2005;41(10):909–20.
[5] William S, Luigi P, Kang L. Nonlinear modeling of NO_x emission in a coal-fired power generation plant. In: 43rd IEEE conference on decision and control. Atlantis, Paradise Island, Bahamas; 2004. p. 3850–5.
[6] Qin SJ, Yue H, Dunia R. Self-validating inferential sensors with application to air emission monitoring. Ind Eng Chem Res 1997;36:1675–85.
[7] Flynn D, Ritchie J, Cregan M. Data mining techniques applied to power plant performance monitoring. In: 16th IFAC world congress, Prague; 2005.
[8] Kalogirou SA. Artificial intelligence for the modeling and control of combustion processes: a review. Progr Energy Combust Sci 2003;29(6):515–66.
[9] Chong AZS, Wilcox SJ, Ward J. Neural network models of the combustion derivatives emanating from a chain grate stoker fired boiler plant. In: Proceedings of the IEEE seminar advanced sensors and instrumentation systems for combustion processes; 2000. p. 6/1–6/4.
[10] Hao Z, Kefa C, Jianbo M. Combining neural network and genetic algorithms to optimize low NO_x pulverized coal combustion. Fuel 2001;80(15):2163–9.
[11] Luo X, Shao H. Developing soft sensors using hybrid soft computing methodology: a nerofuzzy system based on rough set theory and genetic algorithms. Soft Computing – A Fusion of Foundations. Methodologies Appl 2006;10(1):54–60.
[12] Kusiak A, Song Z. Combustion efficiency optimization and virtual testing: a data-mining approach. IEEE Trans Ind Inform 2006;2(3):176–84.

[13] Schölkopf B, Smola AJ. Learning with Kernels: support vector machines, regularization, optimization, and beyond. Cambridge, MA: MIT Press; 2002.
[14] Smola AJ, Schölkopf B. A tutorial on support vector regression. Statist Comput 2004;14(4):199–222.
[15] Ma JS, Theiler J, Perkins S. Accurate on-line support vector regression. Neural Comput 2003;15:2683–703.
[16] Platt JC. Using analytic QP and sparseness to speed training of support vector machines. In: Proceedings of the 1998 conference on advances in neural information processing systems II; 1998. p. 557–63.
[17] Shevade SK, Keerthi SS, Bhattacharyya C, Murthy KRK. Improvements to the SMO algorithm for SVM Regression. IEEE Trans Neural Networks 2000;11(5):1188–93.
[18] Flake GW, Lawrence S. Efficient SVM regression training with SMO. Mach Learn 2002;46:271–90.
[19] Kaisa MM. Nonlinear multiobjective optimization. Boston, Massachusetts: Kluwer Academic Publishers; 1999.
[20] Rosenberg RS. Simulation of genetic populations with biochemical properties. Ph.D. Thesis. Ann Harbor, Michigan: University of Michigan; 1967.
[21] Rudolph G. On a multi-objective evolutionary algorithm and its convergence to the Pareto set. In: Proceedings of the 5th IEEE conference on evolutionary computation. Piscataway, New Jersey: IEEE Press; 1998. p. 511–6.
[22] Thomas B. Evolutionary algorithms in theory and practice: evolution strategies, evolutionary programming, genetic algorithms. Oxford University Press; 1996.
[23] Fleming PJ, Purshouse RC. Evolutionary algorithms in control systems engineering: a survey. Control Eng Pract 2002;10(11):1223–41.
[24] Schaffer JD. Multiple objective optimization with vector evaluated genetic algorithms. In: Proceedings of the first international conference on genetic algorithms; 1985. p. 93–100.
[25] Zitzler E, Deb K, Thiele L. Comparison of multiobjective evolutionary algorithms: empirical results. Evol Comput 2000;8(2):173–95.
[26] Jeffrey H, Nicholas N, David EG. A niched Pareto genetic algorithm for multiobjective optimization. In: Proceedings of the first IEEE conference on evolutionary computation, IEEE world congress on computational intelligence, vol. 1. Piscataway, New Jersey, 1994. p. 82–7.
[27] Srinivas N, Deb K. Multiobjective optimization using nondominated sorting in genetic algorithms. Evol Comput 1994;2(3):221–48.
[28] Deb K, Pratap A, Agrawal S, Meyarivan T. A fast elitist non-dominated sorting genetic algorithm for multi-objective optimization: NSGA-II. IEEE Trans Evol Comput 2002;6(2):182–97.
[29] ASME PTC 4 Fired Steam Generators. American Society of Mechanical Engineers; 1998.
[30] Marshall L, Afonso R, Tavoulareas S, Stallings J. Prediction and mitigation of air preheater fouling due to ammonium bisulfate. In: Proceedings of the EPRI-DOE-EPA combined power plant air pollutant control symposium: the MEGA symposium. Chicago; 2001.
[31] Sarunac N, Levy E. RPHMT – air preheater metal temperature code, vol. 1.1. EPRI Project RP1691/2153; April 1989.